

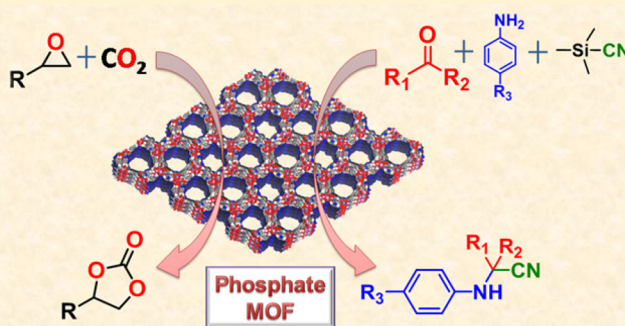
From Zn(II)-Carboxylate to Double-Walled Zn(II)-Carboxylato Phosphate MOF: Change in the Framework Topology, Capture and Conversion of CO₂, and Catalysis of Strecker Reaction

Mayank Gupta, Dinesh De, Kapil Tomar, and Parimal K. Bharadwaj*

Department of Chemistry, Indian Institute of Technology Kanpur, Kanpur 208016, India

S Supporting Information

ABSTRACT: The ligand H₂L has been built by linking an imidazole moiety to the 5-position of isophthalic acid. It forms two types of porous frameworks, {[Zn(L)]·2DMF·2H₂O}_n (1) and {[[(CH₃)₂NH₂][Zn₂(L)(H₂O)PO₄]·2DMF}_n (2). 1 is a porous neutral framework and has *rtl rutile 3,6-conn* topology, while 2 is an organo-metallophosphate anionic porous framework with double-walled hexagonal channels. Framework 1' (desolvated) exhibits moderate CO₂ adsorption (58 cc g⁻¹ at 273 K, 1 bar), whereas 2' (desolvated) shows a microporous nature with a high adsorption of CO₂ (111.7 cc g⁻¹ or 22 wt % at 273 K, 1 bar). Interestingly, this adsorbed CO₂ could be converted very efficiently to cyclic carbonates under mild conditions using 2' as the catalyst in the presence of tetrabutylammonium bromide as the cocatalyst. The presence of open metal sites in 2' makes it an efficient heterogeneous catalyst for solvent-free three-component Strecker reaction using various aldehydes/ketones together with amines and trimethylsilyl cyanide in high yields at room temperature. The straightforward experimental and product isolation procedure along with easy recovery and reusability of the catalyst provided an attractive route for the synthesis of α -amino nitriles.



INTRODUCTION

Syntheses of nanoporous materials¹ with extended network topologies have been emerging as very powerful platforms for various applications such as gas storage,² separation,³ sensing,⁴ catalysis,⁵ and so on. These porous materials can largely be divided into two major categories, one with only inorganic frameworks,⁶ such as zeolites, germinates, and phosphate based metal oxides; and the other one is metal–organic hybrid frameworks or the porous coordination polymers.⁷ In this regard, porosity in phosphate based metal oxides (MPOs) has been thoroughly investigated.⁸ Recently, multidentate organic ligands, like oxalate⁹ and 4,4'-bpy¹⁰ type moieties, have been incorporated into MPOs to obtain structural diversity in the resultant organo-metallophosphate frameworks (OMPOs). Unfortunately, very few OMPOs have shown a porous nature which could be utilized for application purposes.¹¹

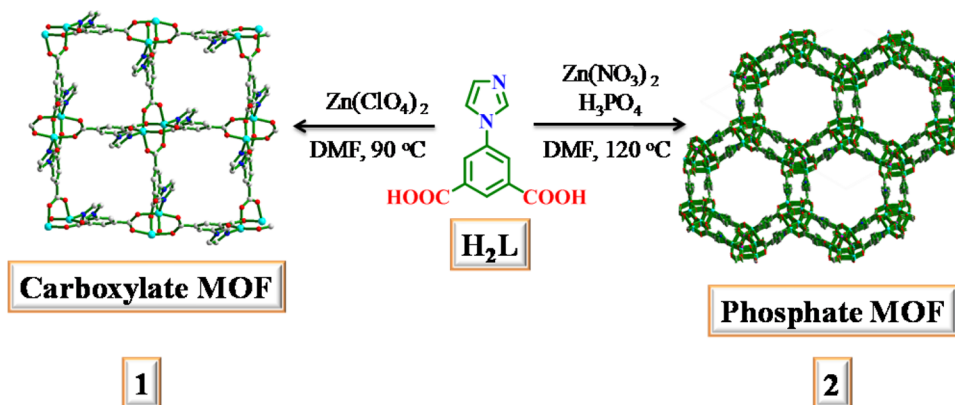
Aromatic carboxylates have been found to be very effective building blocks for obtaining porous metal–organic frameworks (MOFs).¹² Incorporation of the carboxylates into MPOs to obtain porous hybrid materials is very low in number and has been achieved only by Wang and co-workers in two separate reports.^{13,14} These materials, like other MPOs, have been synthesized with the help of 4,4'-bipyridine templates which remain in the pores of frameworks as cationic species and were difficult to remove to obtain porous frameworks. We thought to combine these moieties into one ligand, and the imidazole-substituted

isophthalic acid¹⁵ H₂L (Scheme 1) was chosen to construct a phosphate based metal organic framework.

Herein, we have successfully achieved the synthesis of two categories of porous frameworks (Scheme 1) from the same ligand, L²⁻ (hereafter L), {[Zn(L)]·2DMF·2H₂O}_n (1), a metal–organic framework, and {[[(CH₃)₂NH₂][Zn₂(L)(H₂O)PO₄]·2DMF}_n (2), an organo-metallophosphate anionic framework. Compound 2 is the first OMPO which is synthesized without any external templating molecule which generally obstructs the porosity of the framework.

Both the frameworks can be activated to obtain porous structures, 1' and 2', without breakdown of the overall architecture. Gas adsorption and heterogeneous catalytic activities of the frameworks afforded interesting results. Compared to 1', the framework 2' afforded greater CO₂ adsorption and its conversion to cyclic carbonates that are valuable as precursors for having polycarbonates, aprotic polar solvents, pharmaceutical/fine chemical intermediates, and in many biomedical applications.¹⁶ The framework 2', having open metal sites, exhibited efficient heterogeneous catalytic activity for solvent-free three-component Strecker reaction using various aldehydes/ketones together with amines and trimethylsilyl cyanide (TMS-CN) to afford the corresponding α -amino nitriles in high yields at room temperature. The Strecker reaction is one of the most efficient and

Received: September 23, 2017

Scheme 1. Structure of the Ligand H_2L and Synthetic Scheme of Porous Frameworks, 1 and 2

straightforward methods for the synthesis of α -amino nitriles,¹⁷ which are very useful precursors for the synthesis of α -amino acids and various nitrogen-containing heterocycles such as imidazoles and thiadiazoles, etc.¹⁸

EXPERIMENTAL SECTION

Materials and Measurements. All chemicals were reagent grade quality obtained from either Aldrich or TCI and used without further purification. All solvents were procured from S. D. Fine Chemicals, India. These solvents were purified following standard methods prior to use. The details of spectroscopic techniques and X-ray structural studies are provided in the [Supporting Information](#).

Synthesis of 5-(1H-imidazol-1-yl)isophthalic acid (H_2L). The ligand was synthesized according to a procedure reported in the literature.¹⁵

Synthesis of $\{[\text{Zn}(\text{L})] \cdot 2\text{DMF} \cdot 2\text{H}_2\text{O}\}_n$ (1). H_2L (30 mg, 0.13 mmol) and $\text{Zn}(\text{ClO}_4)_2 \cdot 6\text{H}_2\text{O}$ (60 mg, 0.16 mmol) were mixed with 3 mL of DMF in a 5 mL Teflon vessel and heated at 90 °C for 72 h. After cooling to room temperature, the resulting colorless block-shaped crystals were harvested and washed repeatedly with DMF, followed by acetone, and air-dried to give a high yield of 80% (based on the ligand). Anal. Calcd for $\text{C}_{17}\text{H}_{24}\text{N}_4\text{O}_8\text{Zn}$: C, 42.74; H, 5.06; N, 11.73%. Found: C, 42.98; H, 5.21; N, 11.69%. IR (cm^{-1}): 3424 (broad), 3138 (s), 1628 (s), 1584 (s), 1511 (s), 1434 (s), 1382 (m), 1320 (s), 1269 (m), 1140 (w), 1118 (m), 1071 (s), 1004 (w), 945 (m).

Synthesis of $\{[(\text{CH}_3)_2\text{NH}_2][\text{Zn}_2(\text{L})(\text{H}_2\text{O})\text{PO}_4] \cdot 2\text{DMF}\}_n$ (2). H_2L (30 mg, 0.13 mmol), $\text{Zn}(\text{NO}_3)_2 \cdot 6\text{H}_2\text{O}$ (60 mg, 0.20 mmol), and H_3PO_4 (85%, 20 μL) were mixed with 3 mL of DMF in a 5 mL Teflon vessel and heated at 120 °C for 72 h. After cooling to room temperature, the resulting colorless block-shaped crystals were harvested and washed repeatedly with DMF, followed by acetone, and air-dried to give a high yield of 83% (based on the ligand). Anal. Calcd for $\text{C}_{19}\text{H}_{28}\text{N}_5\text{O}_{11}\text{PZn}_2$: C, 34.36; H, 4.25; N, 10.54%. Found: C, 34.53; H, 4.39; N, 10.61%. IR (cm^{-1}): 3434 (broad), 3111 (m), 2449 (bw), 2041 (bw), 1669 (s), 1623 (s), 1593 (w), 1402 (s), 1334 (m), 1242 (m), 1166 (w), 1109 (w), 1064 (s), 1026 (w).

General Procedure for the Coupling of Epoxides with CO_2 . Catalyst (2) was activated by heating at 150 °C for a period of 8 h after soaking 5 days in the methanol, which was changed two times per day with fresh methanol. The activation temperature was chosen from TG data in order to remove all traces of solvent inside the pore. Reactions were carried out in a Schlenk tube with stirring at 30 or 70 °C depending on the substrate, and CO_2 (99.999%) bubbling. Epoxide (20 mmol), catalyst 2' (10 wt %), and cocatalyst TBAB (1 mmol) were added. Upon completion, the reaction mixture and catalyst were separated by filtration to obtain a crude compound. This crude mixture was given for ^1H NMR (in CDCl_3) for calculating the yield.

General Procedure for the Strecker Reactions. Catalyst (2) was activated as described above. Then, the mixture of ketone/aldehyde, amine, and trimethylsilyl cyanide (TMSCN) was added to a Schlenk tube (1 mmol of ketone, 1 mmol of amine, and 1.2 mmol of TMSCN),

where the catalyst 2' (10 wt %) has been previously introduced. The mixture (in solvent-free conditions) was stirred at 25 °C between 0.5 and 18 h depending on the substrate, under a N_2 atmosphere. When the reaction was completed, 10 mL of DCM was added to the mixture in order to dissolve the Strecker–aminonitrile. The mixture was then filtered and washed to afford the crude product. It was further purified with a small pad of silica using hexane/ethyl acetate as an eluent.

RESULTS AND DISCUSSION

The solvothermal reaction of $\text{Zn}(\text{ClO}_4)_2$ at 90 °C with the ligand H_2L in DMF afforded 1, while the solvothermal reaction with $\text{Zn}(\text{NO}_3)_2$ at 120 °C in the presence of phosphoric acid gave an anionic framework 2 with a double-walled rosette structure and large open hexagonal pores (Scheme 1).

Single crystal X-ray analysis revealed that 1 crystallized in the monoclinic space group $P2_1/c$. The asymmetric unit contains one Zn(II) ion, one ligand L^{2-} , two DMF, and two water molecules in the lattice. As shown in Figure 1a, Zn1 center showed penta-coordinated geometry with ligation from four O atoms of two COO^- groups of one ligand and one N atom of the imidazole moiety of another ligand to form a paddle-wheel SBU, $\text{Zn}_2(\text{COO})_4\text{N}_2$. The distance between the two $\text{Zn} \cdots \text{Zn}$ ions was found to be 3.032 Å. The resulting coordination arrangement of Zn(II) ion and the ligand gave rise to a 3D porous framework with 1D open channels along the crystallographic a -axis with channel dimensions of $\sim 12 \times 7 \text{ Å}^2$ (Figure 1b). The channels in the framework are filled with DMF and water solvent molecules. The total potential solvent accessible void volume of 1 was calculated to be 51.8% ($956.1 \text{ Å}^3 / 1847.3 \text{ Å}^3$) when DMF and water solvent molecules were removed from the lattice. Topological analysis (Figure 1c) with TOPOS revealed that the $\text{Zn}_2(\text{COO})_4\text{N}_2$ paddle-wheel SBU could be considered as a six connected node and the ligand L as a three connected node. This made the framework a 3,6-c binodal net having point symbol $\{4.6^2\}_2\{4^2.6^{10}.8^3\}$, assignable to the topological type, *rtl rutile* 3,6-conn (topos&RCSR.ttd).

On the other hand, the phosphate based anionic framework 2 crystallized in the rhombohedral space group $R\bar{3}$, and the asymmetric unit consisted of two Zn(II) ions, one L, one PO_4^{3-} anion, one coordinated water and disordered solvent molecules, DMF and $(\text{CH}_3)_2\text{NH}_2$ (DMA) cations. Two carbon atoms of the imidazole moiety were found to be disordered over two positions with assigned occupancies. The solvent and DMA cations are too disordered to be modeled and hence were removed using SQUEEZE. Structural analysis revealed that both Zn1 and Zn2 acquire five-coordinate geometry (Figure 2a) with different coordination environments. Zn1 was coordinated from two O

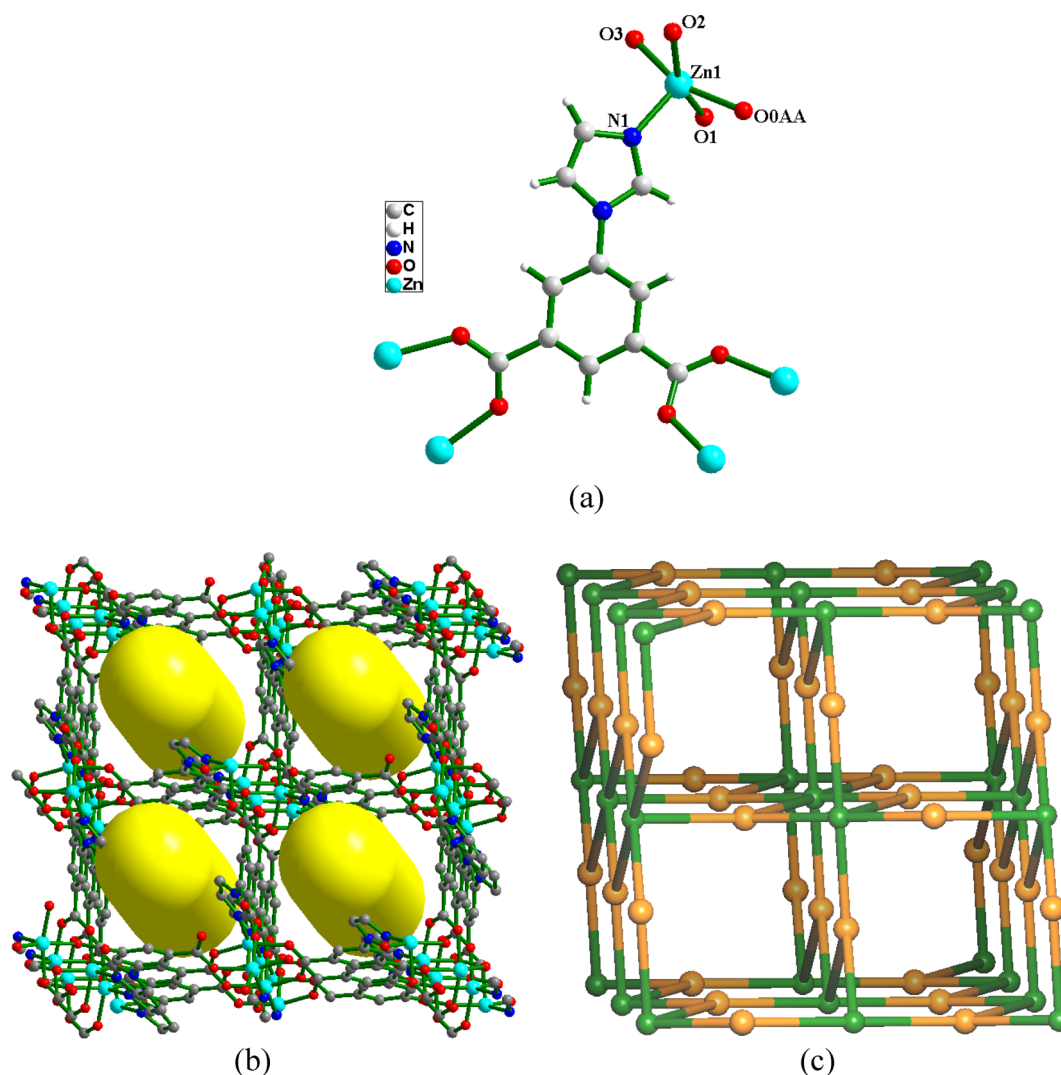


Figure 1. (a) Coordination environment of Zn(II) in **1** and coordination modes of **L**, (b) 3D view of **1** showing the open channels, (c) 3,6-c net of **1** with *rtl rutile 3,6-conn* topology.

atoms of one COO^- group, two O atoms of the PO_4^{3-} anion, and one N atom of the imidazole group, while Zn2 showed ligation from two O atoms of one COO^- group, two O atoms of the PO_4^{3-} anion, and one from a coordinated water molecule. Charge balancing calculations revealed that a total of 4+ charge came from two Zn(II) ions while a total of 5− charge provided by two COO^- and one PO_4^{3-} . Finally, one more positive charge to balance came from a DMA cation originating from the decomposition of DMF solvent during the solvothermal reaction.¹⁹ The presence of DMA cations in the channels was further confirmed by TGA, IR, and elemental analysis studies (see the [Supporting Information](#)).

Structural analysis of **2** revealed that Zn(II) and PO_4^{3-} ions formed a continuous 1D chain along the crystallographic *c*-axis (Figure 2b) connected by the ligand **L** to form double-walled hexagonal channels (Figure 2c,d) with the window size of $\sim 15 \times 16 \text{ \AA}^2$ and, furthermore, formed an interesting 3D framework with a rosette structure. The large hexagonal channels were filled up with DMF molecules and DMA cations. The total potential solvent accessible void volume of **2** was found to be 42.5% ($4477 \text{ \AA}^3/10532 \text{ \AA}^3$). The framework contained coordinated water molecules inside the walls of the channels. Upon heating, the coordinated water molecules could be removed to obtain

activated framework, **2'**, with open metal sites as a potential candidate for gas adsorption and heterogeneous catalysis.

TGA measurements for **1** and **2** were carried out to examine the thermal stability of the networks. The TGA curve of the as-synthesized sample of **1** showed a weight loss of 38% (calculated 38.1%) between 50 and 350 °C corresponding to the loss of all solvent molecules in the cavities. Thereafter, a sharp weight loss was observed that corresponded to the decomposition of the framework (Figure S2). For **2**, the sample showed a weight loss of 32% (calculated 31.7%) between 50 and 275 °C corresponding to the loss of all solvent molecules in the cavities along with the loss of coordinated water molecules. Thereafter, a sharp weight loss indicated collapsing of the framework. Phase purity of the synthesized frameworks was analyzed by PXRD measurements of the as-synthesized samples of **1** and **2**. The experimental PXRD patterns for the as-synthesized compounds were in good agreement with the simulated patterns of **1** and **2**. The methanol exchanged materials were heated under high vacuum at 150 °C for 8 h to generate the activated compounds, **1'** and **2'**. The crystalline nature of the evacuated material was also confirmed by powder XRD (Figures S3 and S4) measurements in which no significant shift or broadening of peaks were observed compared to the as-synthesized materials, **1** and **2**.

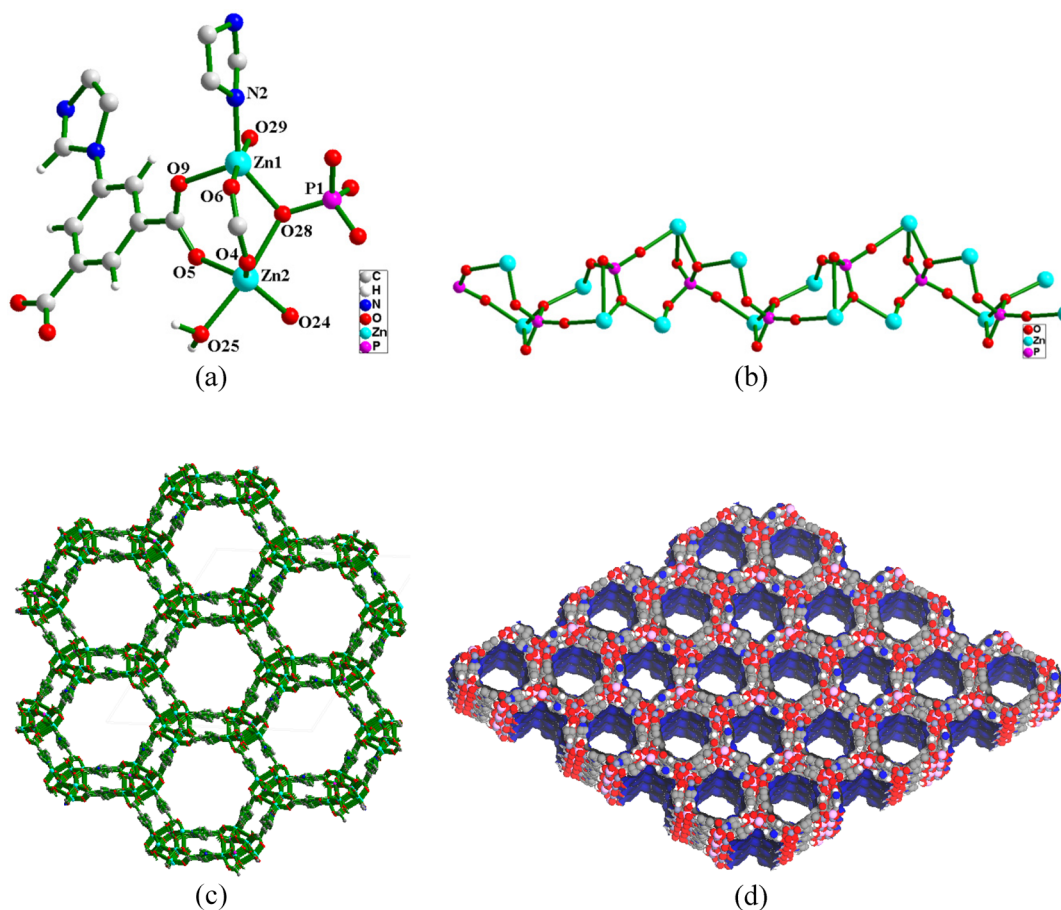


Figure 2. (a) Coordination environment of Zn(II) in **2**, (b) continuous 1D chain formed by Zn(II) ion and PO_4^{3-} anion along the c -axis, (c, d) views of **2** showing the double-walled hexagonal channels along the c -axis.

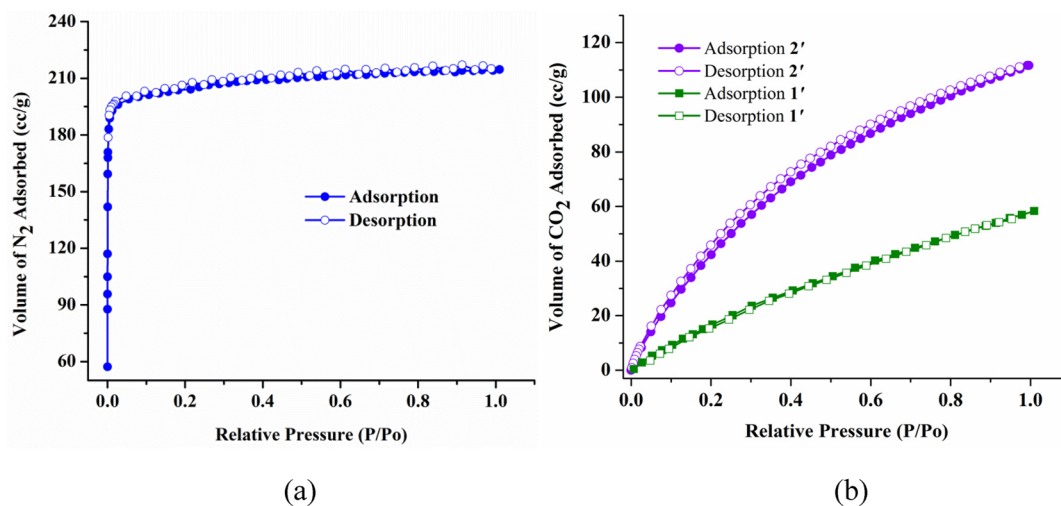


Figure 3. (a) N_2 sorption curve of **2'** at 77 K, (b) CO_2 sorption curves of **1'** and **2'** at 273 K.

Gas Adsorption Studies. The considerable porosity and thermally robust nature of **1** and **2** along with the presence of open metal sites prompted us to study the gas adsorption studies. Activation of **1** and **2** was achieved by keeping the sample in anhydrous methanol for 5 days, followed by heating at 150 °C under high vacuum for 8 h, to produce guest-free **1'** and **2'**. The guest-free frameworks were first subjected to N_2 sorption studies at 77 K. For **1'**, N_2 uptake (Figure S5) was negligible (3.8 cc g^{-1}),

whereas **2'** showed a comparably higher uptake with a maximum uptake of 214.7 cc g^{-1} (Figure 3a). The low N_2 uptake in **1'** can be due to the large kinetic diameter of N_2 (3.6 \AA) than CO_2 (3.3 \AA). Furthermore, the low kinetic energy of the N_2 molecules at 77 K does not allow entering of the small windows of **1'**. Therefore, the BET surface area for **1'** was calculated based on the CO_2 sorption isotherm at 273 K. The Brunauer–Emmett–Teller (BET) surface areas for **1'** and **2'** were estimated to be $215 \text{ m}^2 \text{ g}^{-1}$

(from CO₂ adsorption isotherm) and 750 m² g⁻¹ (from N₂ adsorption isotherms), respectively.

Further, the CO₂ adsorption studies of **1'** and **2'** revealed that the isotherms were quite similar and showed complete reversibility and no hysteresis with a type I adsorption curve (Figure 3b). Sample **1'** showed adsorption of CO₂ gas at 273 K with a maximum uptake of 58 cc g⁻¹ at 1 bar pressure, whereas the uptake value for **2'** was 111.7 cc g⁻¹ at 1 bar pressure. Higher adsorption of N₂ and CO₂ for compound **2'** could be attributed to the open metal sites and larger open channels in the framework.

Catalytic Studies. Cycloaddition of CO₂ to Epoxides for the Synthesis of Cyclic Organic Carbonates. The cycloaddition reaction between CO₂ and epoxides comprises one of the most efficient examples of artificial CO₂ fixation as this reaction is a 100% atom-economic. This fixation of CO₂ is advantageous compared to conventional syntheses using the highly toxic and corrosive phosgene.^{20,21} Because of these advantages, this reaction has been studied extensively.²² In general, for the CO₂ fixation reaction using common catalysts such as metal–salen complexes, metal oxides, and zeolites, high pressure and/or temperature is needed.²³ Recently, few MOFs have been used as promising and efficient catalysts for the conversion of captured CO₂ to cyclic carbonates.²⁴

Given the significant CO₂ uptake capacity and highly robust nature of **2'**, we performed the cycloaddition reaction of CO₂ to epoxides using the coordinatively unsaturated Zn(II) Lewis acidic sites. **2'** in the presence of tetra-*n*-*tert*-butylammonium bromide (TBAB) as a cocatalyst was found to effectively convert a variety of substituted terminal epoxides to the corresponding cyclic carbonates in excellent yields (Table 1). This included epoxides containing aliphatic, aromatic, electron-withdrawing, and electron-donating substituents. In the case of the internal epoxide (Table 1, entry 7), the yield was relatively lower (68% after 22 h). Meanwhile, in a control reaction in the absence of the cocatalyst TBAB, the cycloaddition reaction of CO₂ to epichlorohydrin catalyzed by **2'** yielded only 4% cyclic carbonate after 32 h (Table 1, entry 8). Furthermore, in the absence of **2'**, the same reaction catalyzed by the cocatalyst TBAB alone gave a 9% yield (Table 1, entry 9). Yet, when the catalyst **2'** and cocatalyst TBAB were combined together, a facile reaction occurred (Table 1, entry 1).

To confirm the heterogeneous nature, the hot filtration method was applied.²⁵ The reaction using epichlorohydrin as substrate was stopped by hot filtration of the catalyst at partial conversion (~56%) after dilution with dichloromethane. No further significant reaction occurred if the filtrate was allowed to continue at the same reaction condition (Figure S6). To probe the reusability of the catalyst **2'**, a series of catalytic cycles were examined using epichlorohydrin as substrate. In each cycle, the catalyst **2'** was recovered by simple filtration, washed with methanol, dried under vacuum, and then subjected to a second run of the reaction using the same substrates. The yields in 4 runs were almost the same (Figure S7). The recyclability of the catalyst makes the reaction economically and practically relevant for commercial applications. Notably, the framework integrity of catalyst **2** was sustained after each cycle, as shown by PXRD (Figure S4). Formation of the desired cyclic carbonates was confirmed by the ¹H NMR (Figures S8–S14).

The proposed mechanism of the cycloaddition of CO₂ to epoxides in the presence of Lewis acidic transition metal catalysts and quaternary ammonium salts as cocatalysts has been extensively explored.²⁶ The MOF presents a high activity on CO₂ conversion due to its exposed Lewis acid Zn sites. As shown in

Table 1. Cycloaddition of CO₂ and Various Epoxides Catalyzed by **2'** in the Presence of TBAB^a

Entry	Epoxide	Product	Temperature (°C)	Time(h)	Conversion ^b %
1			70	12	>99
2			30	12	>99
3			70	12	>99
4			70	12	>99
5			70	12	88
6			30	12	68
7			70	22	68
8			70	32	4 ^c
9			70	32	9 ^d

^aReaction conditions: epoxide (20 mmol), catalyst (10 wt %, 1.85 mol % for epichlorohydrin as substrate), TBAB (1 mmol). ^bConversion was evaluated from the ¹H NMR spectra by integration of epoxide versus cyclic carbonate peaks (see the Supporting Information). ^cCatalyzed by **2'** only. ^dCatalyzed by the cocatalyst TBAB alone.

the Scheme S1, it was suggested that the epoxide first coordinates on a Zn center. Subsequently, the Br⁻ produced from *n*Bu₄NBr attacks the less-hindered carbon atom of the epoxide to open the three-membered epoxy ring. Finally, CO₂ inserts to form an alkyl carbonate anion, which subsequently undergoes ring-closing to form the cyclic carbonate product with the regeneration of the catalyst.

One-Pot Synthesis of α -Amino Nitriles by Three-Component Strecker Reaction. Further, we found that **2'** was a highly powerful and recyclable catalyst for the three-component Strecker reaction of ketones, in good to excellent yields under solvent-free conditions. This reaction is a direct and viable method for synthesis of α -amino nitriles which are versatile building blocks for synthesis of α -amino acids and their derivatives.

We started by testing the catalytic activity of **2'** in the three-component reaction between acetophenone, trimethylsilyl cyanide (TMSCN), and aniline. A catalytic amount of **2'** was placed in a Schlenk tube, followed by addition of three reactants. The reaction was performed in a solvent-free state at room temperature. The results of the reaction are summarized in Table 2. The increment of the reaction was monitored by TLC analysis. The catalyst was separated by filtration, washed with chloroform and methanol, followed by drying under vacuum at 100 °C for 5 h, to regenerate the active catalyst. The integrity of the framework was maintained even after four cycles of the reaction, as confirmed by the PXRD of the recovered catalyst (Figure S15), while the catalytic activity was almost unchanged (Figure S16). Formation of the desired product, α -amino nitrile, was confirmed by the ¹H NMR and ¹³C NMR data (Figures S17–S38). The results of the catalytic activity of **2'** (Table 2) revealed that both electron-withdrawing as well as electron-donating groups attached to ketone molecules gave good yield.

Table 2. Results Obtained for the Strecker Reaction Catalyzed by 2'^a

Entry	Aldehyde/Ketone	Amine	Product	Time (h)	Yield ^b %
1				0.5	99
2				7	89
3				7	85
4				7	94
5				7	88
6				7	88
7				18	82
8				18	84
9				12	86
10				12	83
11				12	90

^aReaction conditions: ketone (1 mmol), amine (1 mmol), TMS-CN (1.2 mmol), and cat. 2' (10 wt %, 2.4 mol % for acetophenone as substrate) at 25 °C. ^bIsolated yields.

The proposed mechanism (Scheme S2) for one-pot Strecker reaction is similar as that described by Monge et al.²⁷ The reaction involves the formation of an imine intermediate between the activated carbonyl and the amine derivative, followed by attack of the cyano group to the imine carbon atom. The heterogeneous nature of 2' was ensured by the hot filtration method. After allowing the reaction to go for 3 h taking acetophenone and aniline as substrates, the solid 2' was separated from the reaction mixture by filtration and the mother liquor was transferred to an empty Schlenk flask. The reaction did not progress (Figure S39) at all, proving that the catalyst 2' was necessary and there was no leaching.

CONCLUSIONS

In summary, we showed that the same ligand L formed two categories of porous frameworks: one was a neutral framework, 1,

while the other was an organo-metallophosphate anionic framework, 2. The activated framework 2' exhibited superior N₂ and CO₂ adsorption properties compared to 1'. In addition to this, 2', having Lewis acidic open metal sites located in the channel walls, was an effective catalyst for the cycloaddition of CO₂ to epoxides and one-pot synthesis of α -amino nitriles from a variety of aldehydes/ketones together with amines and trimethylsilyl cyanide. This catalyst 2' was in particular highly stable and could be reused in several successive runs with no considerable loss of activity and with no significant structural change.

ASSOCIATED CONTENT

Supporting Information

The Supporting Information is available free of charge on the ACS Publications website at DOI: 10.1021/acs.inorgchem.7b02443.

Materials and methods, X-ray structural studies, IR spectra, TGA, PXRD, NMR spectra, schemes, and additional figures (PDF)

Accession Codes

CCDC 1575928 and 1575929 contain the supplementary crystallographic data for this paper. These data can be obtained free of charge via www.ccdc.cam.ac.uk/data_request/cif, or by emailing data_request@ccdc.cam.ac.uk, or by contacting The Cambridge Crystallographic Data Centre, 12 Union Road, Cambridge CB2 1EZ, UK; fax: +44 1223 336033.

AUTHOR INFORMATION

Corresponding Author

*E-mail: pkb@iitk.ac.in.

ORCID

Parimal K. Bharadwaj: 0000-0003-3347-8791

Notes

The authors declare no competing financial interest.

ACKNOWLEDGMENTS

We gratefully acknowledge the financial support received from the DST and MNRE, New Delhi, India (to P.K.B.), and SRF from the University Grants Commission (UGC), New Delhi, India, to M.G. D.D. thanks IIT Kanpur for a Research Associate fellowship. YSF to K.T. from SERB (YSS/2015/001088/CS), New Delhi, India.

REFERENCES

(1) Yang, X.-Y.; Chen, L.-H.; Li, Y.; Rooke, J. C.; Sanchez, C.; Su, B.-L. Hierarchically porous materials: synthesis strategies and structure design. *Chem. Soc. Rev.* **2017**, *46*, 481–558.

(2) Makal, T. A.; Li, J.-R.; Lu, W.; Zhou, H.-C. Methane storage in advanced porous materials. *Chem. Soc. Rev.* **2012**, *41*, 7761–7779.

(3) Yu, J.; Xie, L.-H.; Li, J.-R.; Ma, Y.; Seminario, J. M.; Balbuena, P. B. CO₂ Capture and Separations Using MOFs: Computational and Experimental Studies. *Chem. Rev.* **2017**, *117*, 9674–9754.

(4) Kreno, L. E.; Leong, K.; Farha, O. K.; Allendorf, M.; Van Deyne, R. P.; Hupp, J. T. Metal–Organic Framework Materials as Chemical Sensors. *Chem. Rev.* **2012**, *112*, 1105–1125.

(5) Corma, A. From Microporous to Mesoporous Molecular Sieve Materials and Their Use in Catalysis. *Chem. Rev.* **1997**, *97*, 2373–2420.

(6) Zheng, H.; Gao, F.; Valtchev, V. Nanosized inorganic porous materials: fabrication, modification and application. *J. Mater. Chem. A* **2016**, *4*, 16756–16770.

(7) Maspoch, D.; Ruiz-Molina, D.; Veciana, J. Old materials with new tricks: multifunctional open-framework materials. *Chem. Soc. Rev.* **2007**, *36*, 770–818.

(8) Murugavel, R.; Choudhury, A.; Walawalkar, M. G.; Pothiraja, R.; Rao, C. N. R. Metal Complexes of Organophosphate Esters and Open-Framework Metal Phosphates: Synthesis, Structure, Transformations, and Applications. *Chem. Rev.* **2008**, *108*, 3549–3655.

(9) (a) Kizewski, F. R.; Boyle, P.; Hesterberg, D.; Martin, J. D. Mixed Anion (Phosphate/Oxalate) Bonding to Iron(III) Materials. *J. Am. Chem. Soc.* **2010**, *132*, 2301–2308. (b) Neeraj, S.; Natarajan, S.; Rao, C. N. R. A zinc phosphate oxalate with phosphate layers pillared by the oxalate units. *J. Chem. Soc., Dalton Trans.* **2001**, 289–291.

(10) Fan, J.; Hanson, B. E. Novel Zinc Phosphate Topologies Defined by Organic Ligands. *Inorg. Chem.* **2005**, *44*, 6998–7008.

(11) Vaidhyanathan, R.; Iremonger, S. S.; Shimizu, G. K. H.; Boyd, P. G.; Alavi, S.; Woo, T. K. Competition and Cooperativity in Carbon Dioxide Sorption by Amine-Functionalized Metal–Organic Frameworks. *Angew. Chem., Int. Ed.* **2012**, *51*, 1826–1829.

(12) Zhou, H.-C.; Long, J. R.; Yaghi, O. M. Introduction to Metal–Organic Frameworks. *Chem. Rev.* **2012**, *112*, 673–674.

(13) Liao, Y.-C.; Liao, F.-L.; Chang, W.-K.; Wang, S.-L. A Zeolitic Organo–Metallophosphate Hybrid Material with Bimodal Porosity. *J. Am. Chem. Soc.* **2004**, *126*, 1320–1321.

(14) Huang, S.-H.; Lin, C.-H.; Wu, W.-C.; Wang, S.-L. Network Topology of a Hybrid Organic Zinc Phosphate with Bimodal Porosity and Hydrogen Adsorption. *Angew. Chem., Int. Ed.* **2009**, *48*, 6124–6127.

(15) (a) Cheng, F.; Li, Q.; Duan, J.; Hosono, N.; Noro, S.-i.; Krishna, R.; Lyu, H.; Kusaka, S.; Jin, W.; Kitagawa, S. Fine-tuning optimal porous coordination polymers using functional alkyl groups for CH₄ purification. *J. Mater. Chem. A* **2017**, *5*, 17874–17880. (b) Zhu, S.-L.; Ou, S.; Zhao, M.; Shen, H.; Wu, C.-D. A porous metal–organic framework containing multiple active Cu²⁺ sites for highly efficient cross dehydrogenative coupling reaction. *Dalton Trans.* **2015**, *44*, 2038–2041.

(16) (a) Shaikh, A. A. G.; Sivaram, S. Organic Carbonates. *Chem. Rev.* **1996**, *96*, 951–976. (b) Nicolaou, K. C.; Couladouros, E. A.; Nantermet, P. G.; Renaud, J.; Guy, R. K.; Wrasidlo, W. Synthesis of C-2 Taxol Analogues. *Angew. Chem., Int. Ed. Engl.* **1994**, *33*, 1581–1583. (c) Clements, J. H. Reactive Applications of Cyclic Alkylene Carbonates. *Ind. Eng. Chem. Res.* **2003**, *42*, 663–674.

(17) Strecker, A. Ueber die künstliche Bildung der Milchsäure und einen neuen, dem Glycocol homologen Körper. *Ann. Chem. Pharm.* **1850**, *75*, 27.

(18) Dyker, G. Amino Acid Derivatives by Multicomponent Reactions. *Angew. Chem., Int. Ed. Engl.* **1997**, *36*, 1700–1702.

(19) An, J.; Farha, O. K.; Hupp, J. T.; Pohl, E.; Yeh, J. I.; Rosi, N. L. Metal-adeninate vertices for the construction of an exceptionally porous metal-organic framework. *Nat. Commun.* **2012**, *3*, 604–609.

(20) Fukuoka, S.; Kawamura, M.; Komiya, K.; Tojo, M.; Hachiya, H.; Hasegawa, K.; Aminaka, M.; Okamoto, H.; Fukawa, I.; Konno, S. A novel non-phosgene polycarbonate production process using by-product CO₂ as starting material. *Green Chem.* **2003**, *5*, 497–507.

(21) Sakakura, T.; Kohno, K. The synthesis of organic carbonates from carbon dioxide. *Chem. Commun.* **2009**, 1312–1330.

(22) (a) Mikkelsen, M.; Jorgensen, M.; Krebs, F. C. The teraton challenge. A review of fixation and transformation of carbon dioxide. *Energy Environ. Sci.* **2010**, *3*, 43–81. (b) North, M.; Pasquale, R. Mechanism of cyclic carbonate synthesis from epoxides and CO₂. *Angew. Chem., Int. Ed.* **2009**, *48*, 2946–2948. (c) De, D.; Bhattacharyya, A.; Bharadwaj, P. K. Enantioselective Aldol Reactions in Water by a Proline-Derived Cryptand and Fixation of CO₂ by Its Exocyclic Co(II) Complex. *Inorg. Chem.* **2017**, *56*, 11443–11449.

(23) (a) Decortes, A.; Castilla, A. M.; Kleij, A. W. Salen-Complex-Mediated Formation of Cyclic Carbonates by Cycloaddition of CO₂ to Epoxides. *Angew. Chem., Int. Ed.* **2010**, *49*, 9822–9837. (b) Xie, Y.; Wang, T.-T.; Liu, X.-H.; Zou, K.; Deng, W.-Q. Capture and Conversion of CO₂ at Ambient Conditions by a Conjugated Microporous Polymer. *Nat. Commun.* **2013**, *4*, 1960.

(24) (a) Beyzavi, M. H.; Klet, R. C.; Tussupbayev, S.; Borycz, J.; Vermeulen, N. A.; Cramer, C. J.; Stoddart, J. F.; Hupp, J. T.; Farha, O. K. A Hafnium-Based Metal–Organic Framework as an Efficient and Multifunctional Catalyst for Facile CO₂ Fixation and Regioselective and Enantioselective Epoxide Activation. *J. Am. Chem. Soc.* **2014**, *136*, 15861–15864. (b) Verma, A.; De, D.; Tomar, K.; Bharadwaj, P. K. An Amine Functionalized Metal–Organic Framework as an Effective Catalyst for Conversion of CO₂ and Biginelli Reactions. *Inorg. Chem.* **2017**, *56*, 9765–9771.

(25) Neogi, S.; Sharma, M. K.; Bharadwaj, P. K. Knoevenagel condensation and cyanosilylation reactions catalyzed by a MOF containing coordinatively unsaturated Zn(II) centers. *J. Mol. Catal. A: Chem.* **2009**, *299*, 1–4.

(26) Zalomaeva, O. V.; Chibiryayev, A. M.; Kovalenko, K. A.; Kholdeeva, O. A.; Balzhinimaev, B. S.; Fedin, V. P. Cyclic carbonates synthesis from epoxides and CO₂ over metal–organic framework Cr-MIL-101. *J. Catal.* **2013**, *298*, 179–185.

(27) Aguirre-Díaz, L. M.; Gándara, F.; Iglesias, M.; Snejko, N.; Gutiérrez-Puebla, E.; Monge, M. Á. Tunable Catalytic Activity of Solid Solution Metal–Organic Frameworks in One-Pot Multicomponent Reactions. *J. Am. Chem. Soc.* **2015**, *137*, 6132–6135.